U SCIENCE TECH
FACULTAT DE CIÈNCIES
I TECNOLOGIA
UVIC-UCC

Final Thesis

FGF23: Possible kidney clearance role and time-course of the effects in phosphate homeostasis

Lena Nerea Montaña Ernst

Biotechnology

Advisor: Susanna Bodoy Salvans

Vic, September 2016

Acknowledgments

There are many persons that contributed to this thesis. First of all, I want to give my thanks to Carsten A. Wagner which welcomed my in his group and since the first moment he putted his trust in my, giving me the opportunity to start my own project from 0, and helping me always when needed although his busy schedule.

My special gratitude to Nati Hernando, for his infinite patience showing me new techniques and for his good mood, also in the worst moments. Our scientific discussions have been crucial to grow as scientist.

Thanks to all the Wagner group, they showed me the meaning and the importance of team work and of course for all the coffee times (sometimes really needed). Thanks to make my feel like in home in Switzerland.

I am really happy with my supervisor, Susanna Bodoy, who constantly followed my project although the distance and helped my with the organization and writing of this thesis.

Finally, but not least important, many thanks to my family for supporting all my decisions, and for the blindly trust they always have in my.

All these persons helped me to grow professionally, and even more important, personally. Thanks a lot.

Abbreviations

1,25[OH]2D	1,25-dihydroxyvitamin D (Calcitriol)
ADHR	Autosomal dominant hypophosphatemic rickets
ARHR	Autosomal recessive hypophosphatemic rickets
BBM	Brush border membrane
BNX	Bilateral nephrectomy
CDK	Chronic kidney disease
cFGF23	C-terminal fibroblast growth factor 23
Cyp24a1	1,25-dihydroxyvitamin D3 24-hydroxylase
CYP24A1	24-hydroxylase
CYP27B1	1-alpha-hydroyxylase
ESDR	End-stage renal disease
FGF23	Fibroblast growth factor 23
FGFR	Fibroblast growth factor receptor
FGFs	Fibroblast growth factors
HS	Heparin sulfate
iFGF23	Intact fibroblast growth factor 23
IP injection	Intraperitoneal injection
NaPi	Sodium/phosphate cotransporter
ON	Overnight
PBS	Phosphate buffered saline
pFGF23	Plasma fibroblast growth factor 23
Pi	Inorganic phosphate
PTH	Parathyroid hormone
rhFGF23	Recombinant human fibroblast growth factor 23
RXR	Retinoid X receptor
SPC	Subtilisin-like proprotein convertase
TIO	tumor-induced osteomalacia
UNX	Unilateral nephrectomy
UV light	Ultraviolet light
VDR	Vitamin D receptor
VDREs	Vitamin D responsive elements
XLH	X-linked hypophosphatemic rickets

Index

Abstract

Biotechnology

FGF23: Possible kidney clearance role and time-course effects in the phosphate handling

KEYWORDS: FGF23; phosphate handling; renal clearance; NaPi-IIa

Lena Nerea Montaña Ernst

Susanna Bodoy Salvans, Carsten A. Wagner

Fibroblast growth factor 23 (FGF23) is a bone-derived hormone that regulates renal phosphate reabsorption by decreasing the expression of NaPi-IIa cotransporter in the brush border membrane (BBM) of renal proximal tubules, taking part in a hormonal axis which include vitamin D and parathyroid hormone (PTH) to maintain phosphate and calcium homeostasis. Several studies demonstrated a significant increase in plasma FGF23 levels in diseases which involve kidney failure or in renal nephrectomy, indicating a key role of the kidney in direct or indirect FGF23 clearance. Here we try to demonstrate: 1) if the kidney can directly clear FGF23 and 2) the time-course of the FGF23 effect in phosphate handling. For the first goal, we injected recombinant human FGF23 (rhFGF23) in normal rats and analyzed by immunofluorescence techniques whether we could detect it in kidney: no FGF23 was detected in renal cells, neither at 2 nor at 12 hours post administration probably at least in part of technical issues. For the second objective, blood, urine and kidneys were collected at several intervals after rhFGF23 administration. rhFGF23 showed a peak in plasma 2 h after injection, decreasing to less than a half after 6 h and to almost background levels after18 h. rhFGF23 was not detected in urine at any time point. After 6 h of FGF23 injection a decrease in NaPi-IIa (mRNA and protein) was observed in the kidney, in parallel with an enhanced urinary phosphate excretion. Although NaPi-IIa protein remained reduced 18 h post administration, its mRNA levels as well as urinary excretion of phosphate tended to return to their basal levels. No alterations in plasma phosphate levels were found in any of the groups. Furthermore, vitamin D receptor (VDR) protein expression was transiently decreased in the kidney, whereas no alterations in 24-hydroxylase (CYP24a1) were found. Measurements of FGF23 protein abundance in kidney were not valid, due to technical reasons. Thus, our findings are not conclusive regarding the possibility that FGF23 is filtered in the kidney and excreted in the urine. On the other hand, they indicate that the major action of FGF23 on

phosphate excretion and NaPi-IIa expression takes place 6 h after injection, with urinary phosphate but not NaPi-IIa recovering to basal levels after 18 h.

1. Introduction

1.1 Phosphate homeostasis

Inorganic phosphate is essential for bioenergetics (ATP, GTP), metabolic regulation (e.g., in glycolysis or oxidative phosphorylation), intracellular signaling pathways, cell proliferation (as part of DNA or RNA), and for the integrity of structures as bone matrix and cellular membranes[1–3]. Almost all the phosphorous in humans is found in bone and only a 0.1% exists as inorganic phosphate anion in extracellular fluids [4,5]. However the regulation of this small percent is extremely important since alterations in phosphorous homeostasis are involved in multiple physiopathologic mechanisms and clinical processes[6].

In plasma, phosphate exists in both monovalent ($H_2PO_4^-$) and the divalent (HPO_4^{2-}) form. Based on its pK value of 6.8, at blood pH of 7.4, 72% of plasma phosphate is expected to be present in the divalent and 28% in the monovalent form[2,7]. Deregulation of phosphate balance can manifest either in the form of hypo- or hyper-phosphatemia[4].

Body phosphate homeostasis is regulated by a hormonal counter balanced intestine-bone-kidney axis[4] in which the serum phosphorus concentration is determined by the balance between intestinal absorption of phosphate from the diet (16 mg/kg/day), storage of phosphate in the skeleton (3 mg/kg/day), and excretion of phosphate through the urine (13 mg/kg/day)[2,8]. The major regulatory hormones are parathyroid hormone (PTH), vitamin D and fibroblast growth factor 23 (FGF23)[9].

Inorganic phosphate is absorbed along the entire length of the intestine, with the small intestine having a significantly higher absorption capacity as compared with the colon[10]. Intestinal phosphate transport occurs through 2 distinct mechanisms, a passive transport and an active sodium-dependent transport pathway[8,10]. The passive transport mechanisms generally depend on electrochemical gradients across epithelial layers with actual paracellular movement occurring through tight junction complexes that are formed by the interaction of complementary junctional proteins of neighboring cells[7,10]. In contrast, two families of sodium-dependent phosphate transporters, the SLC34 family [SLC34A1 (or NaPi-IIa), SLC34A2 (or NaPi-IIb) and SLC34A3 (or NaPi-IIc)] and the SLC20 family [SLC20A1 (or PiT-1) and SLC20A2 (or PiT-2)], are responsible for active the transport of extracellular phosphate[10,11]. All the SLCA34 isoforms preferentially transport divalent phosphate, whereas

that the SLC20 proteins preferentially transport monovalent phosphate. That's, among other reasons, why the phosphate transport capacity is strongly pH dependent[11].

The SLC34 family members seem to be the major handlers of sodium-dependent phosphate in the kidney (NaPi-IIa and NaPi-IIc) and the intestine (NaPi-IIb)[10].

In the small intestine of humans and rats, NaPi-IIb is expressed at the luminal brush border membrane of the duodenum and jejunum, whereas in mice is located mostly in ileum[2,7,8]. This cotransporter is mainly up regulated by reduction of dietary phosphate intake[2] and $1,25(OH)_2D$ (calcitriol)[1,2], but several other factors have been shown to specifically or indirectly modulate NaPi-IIb expression and/or sodium-dependent phosphate transport in the intestine. These include epidermal growth factor, thyroid hormones, glucocorticoids, estrogens, metabolic acidosis, matrix extracellular phosphoglycoprotein, and FGF23[2,10].

The kidney is known as the major regulator of phosphate homeostasis[8]. The main site of phosphate reabsorption is the proximal tubule[2], were phosphate ions enter from the tubular lumen across the apical brush-border membrane (BBM) and leave across the basolateral membrane[8].

To date, three distinct transporters have been identified to be expressed in the BBM of the proximal tubule cells: NaPi-IIa, NaPi-IIc and PiT-2[12]. NaPi-IIa and PiT-2 mediate the electrogenic transport of phosphate coupled to three and two Na^+ respectively, whereas NaPi-IIc transports phosphate together with two Na^+ in an electroneutral fashion[2,8,11,12]. A plethora of factors affects renal phosphate reabsorption, among them PTH, dopamine, dietary phosphate intake, glucocorticoids, acid-base status, growth factors, insulin and FGF23[2,8,12].

In this project we focused on NaPi-IIa, because its pattern of expression along the proximal tubules matches the major sites of renal phosphate reabsorption, and its role as the main mediator of this process in rodents has been clearly demonstrated[13,14]. In general, NaPi-IIa regulation occurs mostly on the posttranscriptional level by altering the rate of synthesis and degradation thus changing the amount of NaPi-IIa transporter molecules in the BBM[2,8].

1.2 Fibroblast Growth Factor 23

FGF23 is a 32 kDa protein, predominantly expressed in osteoblasts and osteocytes[4,5,15–21], but also expressed in several other tissues including the spleen, thymus, heart, lung, and muscle[5,22] and it is a member of the fibroblast growth factors (FGFs) family[4,5,16].

While some FGFs (FGF11-14) function as intracellular signaling molecules, most signal in an autocrine/paracrine manner[5,23], except FGF15/19, 21 and 23 that function as endocrine hormones[6,16]. A unique structural feature of these endocrine FGFs is their lack of a heparin-binding domain that is conserved in all autocrine/paracrine FGFs. The heparin-binding domain is critical for FGF function in two ways: first, it binds to heparin sulfate (HS) in the extracellular matrix, thereby posing some restriction to the secretion of FGFs and increasing their local concentration to support the paracrine/autocrine mode of action[6,16,23]; second, HS is essential for FGFR activation[16]. Thus, lack of HS binding sites may be advantageous for facilitating release from their production source but is disadvantageous for FGFR activation at their target organs; endocrine FGFs overcome this handicap by using Klotho proteins instead of HS to enhance receptor binding[16,23].

FGF23 has a hydrophobic signal sequence (24 amino acids), an N-terminal FGF core homology domain (155 amino acids) that interacts with FGF receptors FGFR-1, FGFR-3 or FGFR-4, and a unique C-terminal domain (72 amino acids) that binds to α-klotho[1,15,16,24]. FGF23 binds more avidly to FGFRs in the presence of α-klotho, and triggers intracellular signaling pathways that mediate its biological action[15]. Between the N- and C-terminal domains, there is a subtilisin-like proprotein convertase (SPC) proteolytic cleavage site (RXXR, ^{176}RHTR^{179}), a recognition cleavage site for proteins with endoprotease activity[15,16] (Figure 1.2.1 a). FGF23 circulates in the blood as both active intact FGF23 (iFGF23) and inactive C-terminal (cFGF23) and N-terminal fragments. The cFGF23 binds but does not transactivate the FGFR-Klotho complex and can potentially function as a competitive antagonist and inhibit the action of FGF23[15,16] .

The human FGF23 gene is located on chromosome 12p13, is 10 kb long and contains 3 exons[15]. The 5'-upstream promoter region of the FGF23 gene is highly conserved in the mouse, rat and human genes[15]. The rat and mouse FGF23 amino acid sequences are 72% and 71% homologous to human FGF23, respectively[15].

Mass spectroscopic analyses revealed several Ser and Thr residues present within the 162-228 amino acid region are O-glycosylated[15]. Glycosylation protects from proteolytic cleavage

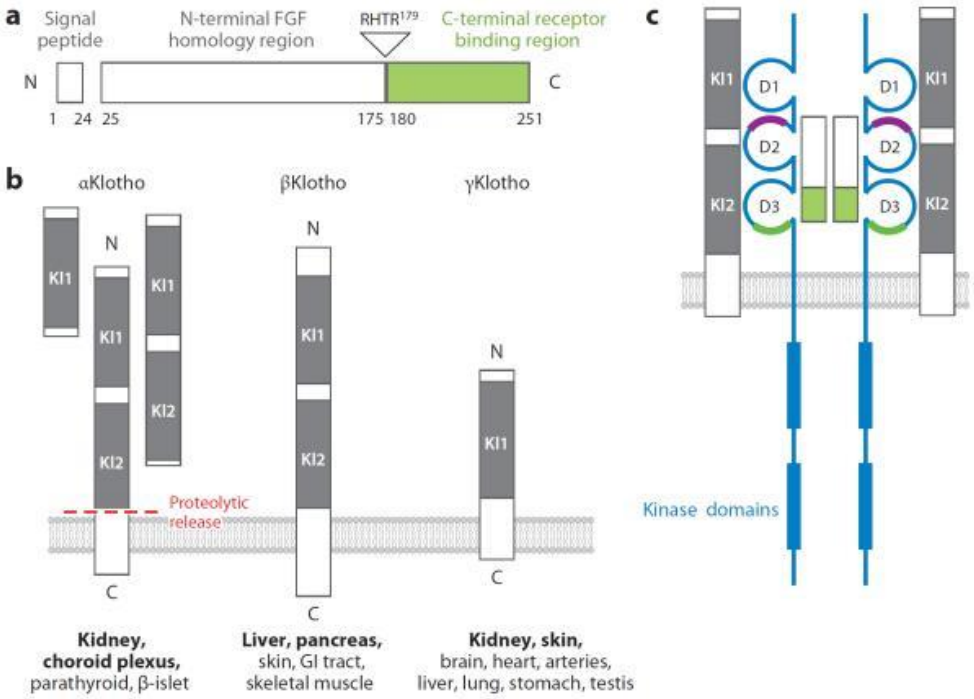

Figure 1.2.1: (a) Structure of FG23 showing the three main domains of this polypeptide. **(b)** Klotho family showing the three members identified to date in the mammalian genome. **(c)** 2FGF23:2FGFR:2αKlotho complex. The FGFR (blue) has three immunoglobulin-like domains (D1, D2, D3) that are stabilized by internal disulfide bridges[16]**.**

FGF23 plays a key role in the regulation of phosphate homeostasis[1,6,16,18,24]. It induces the acute internalization of NaPi-IIa and NaPi-IIc from the BBM and their subsequent degradation, inhibiting phosphate reabsorption in the renal proximal tubule and inducing phosphate exrcretion[5,6,8,15,22,25,26].

It has been observed that in several diseases that involve kidney failure, like chronic kidney disease (CKD), FGF23 levels rise early and quite markedly, leading to think that the kidney has an important role directly or indirectly on the regulation of FGF23.

1.2.1 α-Klotho

α-Klotho is a single-pass transmembrane protein, expressed in the kidney and parathyroid glands, where it forms complexes with FGFR, thus increasing the affinity of the receptor for FGF23 and determining the organ specificity for FGF23 action[6,15,16]. The extracellular domain of α-Klotho has two tandem repeats of β-glucosidase-like domains that are also termed KI domains[16] (Figure1.2.1 b). Klotho and FGFRs form a heterodimeric receptor for FGF23[8].

Soluble forms from α-Klotho can be generated by alternative splicing of its transcript or by proteolytic cleavage of the transmembrane form by β-secretases that release the cleavage fragment into various body fluids including plasma, cerebrospinal fluid, and urine[15,16]. Soluble Klotho acts as a humoral factor and as enzyme regulating several cell surface glycoproteins, including NaPi-IIa[25].

1.2.2 Pathophysiological and clinical implications of FGF23

Disorders that are caused by high circulating levels of FGF23 are characterized by hypophosphatemia, decreased production of 1.25-dihydroxyvitamin D and rickets/osteomalacia[17,23]. This characteristics can be find in ADHR, ARHR, XLH, TIO, and fibrous dysplasia[17,21]. Elevated circulating concentrations of FGF23 are associated with increased mortality in end-stage renal disease (ESRD), coronary artery disease, progression of renal disease and left ventricular hypertrophy, and increased fat mass and dyslipidemia in elderly patients[24].

On the other hand, there are disorders caused by low circulating levels of FGF23, which are characterized by hyperphosphatemia, elevated production of 1.25-dihydroxivitamin D, and soft tissue calcifications[17], like it occurs in humoral calcinosis and hyperostosis, and hyperphosphatemia syndrome[17,21].

1.2.2.1 FGF23 in CKD

CKD is a global public health problem affecting 5-10% of the world's population[16]. CKD leads to disturbances in multiple interrelated hormones that regulate bone and mineral metablosim[27]. Serum concentrations of PTH and FGF23 rise early during the course of CKD in parallel with a decline in vitamin D. Known causes of these hormonal changes include alterations in circulating calcium and phosphate concentrations and inadequate production of vitamin D and Klotho by the failing kidneys[20,28].

Numerous epidemiological studies have reported a robust association between higher plasma FGF23 concentrations and poor patient outcome in CKD populations[22], because it leads to progression to ESRD, cardiovascular disease and death[21]. Elevations in FGF23 levels are one of the earliest manifestations of disordered bone-mineral metabolism in CKD, with deteriorating renal function, even before phosphate and PTH concentrations had become abnormal[6,22–24]. It is unclear whether this represents an adaptive response to phosphate retention, changes in bone mineralization and end-organ resistance due to α-klotho down-regulation or is directly and pathomechanistically related to CKD progression[22].

1.3 Vitamin D_3

Vitamin D_3 (cholecalciferol) is taken in the diet or synthesized in the skin from 7-dehydrocholesterol under the influence of UV light[29,30]. It is first metabolized to 25 hydroxyvitamin D_3 ($25OHD_3$) in the liver, and then converted to the biologically active metabolite form $1,25(OH)_2D_3$ (calcitriol) in the kidney[1,29–32]. This hormonal form of vitamin D_3 affects mineral homeostasis and has numerous other physiological functions including effects on growth of cancer cells and protection against certain immune disorders[29]. CYP2R1 and CYP27A1 encode the two 25-hydroxylases responsible for the formation of $25OHD_3$ in the liver[31–33]. The second hydroxylation reaction, that takes place in the kidney, is mediated by 1α-hydroxylase (CYP27B1)[29–33] (Figure 1.3.1). In contrast,

the enzyme 24-hydroxylase (CYP24A1) is responsible for the catabolism of vitamin D_3 via the C23- and C24-oxidation pathways[34], degrading calcitriol and its precursor[31]. It has both 24-hydroxylase and 23-hydroxylase activity in humans, but the rat enzyme is primarily a 24-hydroxylase[30]. The enzyme CYP24A1 is found in all target tissues and is induced in response to calcitriol[31].

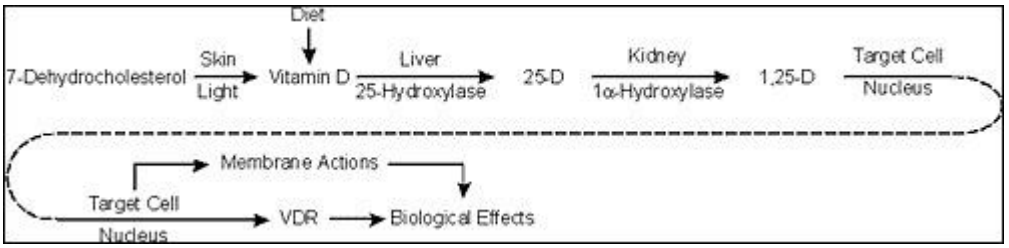

Figure 1.3.1 : The metabolic activation of vitamin D[60].

The biological actions of calcitriol involve regulation of gene expression at the transcriptional level, and are mediated through binding to the vitamin D receptor (VDR), a transcription factor and member of the steroid hormone nuclear receptor family[30] located primarily in the nuclei of target cells[31]. When occupied by calcitriol, VDR interacts with the retinoic X receptor (RXR) to form a heterodimer that binds to vitamin D responsive elements (VDREs) located in the promoter region of genes directly controlled by calcitriol (e.g., FGF23, klotho, NaPi-IIa, CYP27B1 and CYP24A1)[35]. The complete rescue of osteomalacia of the Vdr-null mouse by a diet high in calcium and phosphate suggests that the major role of VDR is the delivery of calcium and phosphate to the bone[36].

The major role of vitamin D in its hormonal form is the elevation of plasma calcium and phosphate levels[31]. It has the capacity to promote the intestinal absorption of calcium, to stimulate bone calcium mobilization and to increase renal reabsorption of calcium in the distal tubule[37–39]; moreover, it stimulates the differentiation of progenitor cells to osteoclasts and encourages bone matrix mineralisation[32,39]. In addition, vitamin D stimulates intestinal absorption of phosphate by increasing the expression of NaPi-IIb in enterocytes, though the NaPi-IIb gene does not contain a canonical VDRE[40]. Diseases that present vitamin D deficiency present symptoms of hypocalcemia and skeletal deformity due to poor mineralization of the bones[32].

1.4 PTH

PTH is an 84-amino acid peptide[25] synthesized as prepro-peptide in the parathyroid glands, and cleaved off in the endoplasmic reticulum resulting in the mature full-length hormone that is stored in secretory vesicles[1], that will release PTH to the blood.

PTH secretion is predominantly regulated by the calcium-sensing receptor (CASR) located in the parathyroid gland, which responds to decrements in serum ionized calcium by increasing secretion of PTH[25]. PTH targets PTHR1 G protein-coupled receptors that are highly expressed in the renal tubules and osteoblasts/osteocytes in bone[8,25].

PTH acts to increase serum calcium by stimulating osteoclasts to resorb bone; in addition and similarly to FGF23 it inhibits renal phosphate reabsorption by decreasing NaPi-IIa, NaPi-IIc and Pit2 expression[41].

1.5 FGF23-Vitamin D-PTH axis

As indicated, phosphate levels are tightly regulated by vitamin D, PTH and FGF23 and these hormones also regulate the serum concentrations of each other (Figure 1.5.1). All these hormones either have their action or are synthesized in the kidney[41].

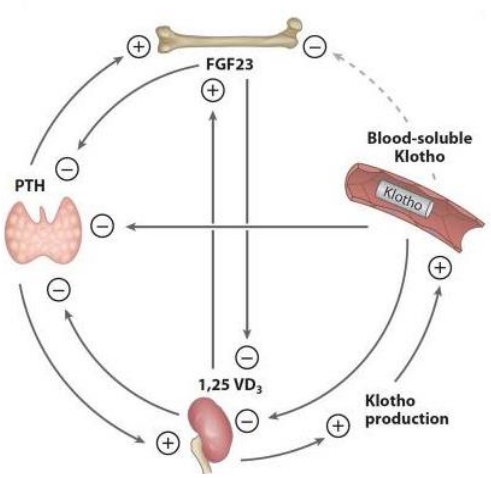

Figure 1.5.1: FGF23-vitamin D-PTH axis[16].

In one hand, vitamin D stimulates FGF23 production through a VDRE that increases FGF23 promoter activity in osteoblasts[17,23], and it also stimulates Klotho production in the kidney[16]. At the same time vitamin D suppresses PTH directly by reducing gene transcription [16,24,42], and perhaps also indirectly by increasing Klotho thus allowing FGF23 to suppress PTH production[15,16,41]. FGF23 reduces renal vitamin D_3 production by a mechanism that has been proposed to involve CYP27B1 inhibition and CYP24A1 stimulation; in addition it also blocks PTH synthesis and/or release from the parathyroid gland[15,25]. PTH activates renal vitamin D production

via CYP27B1 stimulation, and also increases FGF23 production, which has the same action in the kidney[41] as we commented before.

The net effect of this balancing axis is to provide stable calcium and phosphate levels in order to maintain mineral homeostasis.

2. Preliminary results

L. Mace *et al.*[44], studied the role of the kidney in the regulation of FGF23 in the University of Copenhagen and published their results in July 2015. This data was essential to set up our initial hypothesis, and for this reason a brief summary of their results is described below.

They examined the impact of the kidney on the early regulation of intact FGF23 in acute uremia as induced by bilateral or unilateral nephrectomy (BNX and UNX, respectively) in the rat.

They show that BNX resulted in an immediate significant increase in plasma FGF23 levels only 15 min after the intervention and that FGF23 levels remained stable thereafter (Figure 2.1a). This rapid increase is unlikely due to increased transcription of FGF23 in the bone cells, and gene activity studies in the bone indeed showed not significant differences in mRNA expression levels between BNX and control groups. They also demonstrated that the increased FGF23 levels where not due to surgery intervention, since they compared the sham operated group (in which they imitated the manipulation, ischemia, and decapsulation of the kidney during surgery, but the kidney tissue remained intact) with the control and they saw similar FGF23 levels (data not shown).

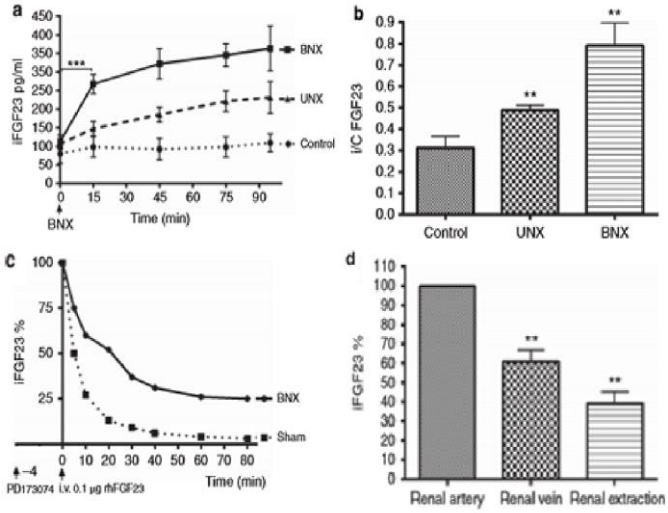

Figure 2.1: (a) plasma levels of iFGF23 after acute BNX or UNX nephrectomy and in the control group. BNX (n = 11), UNX (N = 9), and Control (n = 6). **(b)** The ratio of intact-to-C-terminal FGF23 was measured in the plasma of control, UNX, and BNX rats at 55 min after nephrectomy. (n = 6). **(c)** Disappearance of exogenous recombinant human FGF23 (rhFGF23) in sham and BNX rats; rhFGF23 was administrated after prior inhibition of endogenous FGF23 by PD173074. BNX (n = 6), sham (n = 5) **(d)** FGF23 concentrations in blood samples from renal artery and renal vein.

When intact to C-terminal FGF23 ratio was measured, they observed that the ratio was significantly increased in the BNX group (Figure 2.1b), demonstrating less degradation so the majority of circulating FGF23 in this model of uremia is the intact molecule.

The involvement of the kidneys on FGF23 metabolism was further studied by administration of recombinant human FGF23

(rhFGF23) to normal and BNX rats previously treated with an inhibitor of the FGFR (PD173074) to exclude the interference from endogenous FGF23. They observed a remarkable short half-life of 4.4 min in normal rats and a noticeable slower metabolism in BNX rats, where the half-life was prolonged to 11.8 min (Figure 2.1c). To examine these results further, blood sampling was obtained from renal artery and renal vein demonstrating a significant renal excretion (Figure 2.1d), indicating that the kidney itself clears FGF23.

This data demonstrates that the kidney has a key role in FGF23 metabolism as the half-life of FGF23 was significantly prolonged in BNX animals and the measurements of plasma FGF23 in the renal artery and renal vein suggested a significant renal clearance.

3. Objectives

The two main objectives of the project were:

- Determine whether FGF23 is cleared by the kidney.
- The time course of FGF23 actions on renal phosphate handling.

4. Materials and methods

4.1 Animals

First experiment

The experiment was performed with 16 male Wistar rats weighing 170-200 g. The rats were housed in a temperature-controlled environment with a light/dark circle of 12 hours, with free access to water and food. The rats were kept on a low-phosphate diet (0.1% P_i content; Kliba AG, Switzerland) for 6 days to upregulate the expression of renal Na/phosphate cotransporters NaPi-IIa, NaPi-IIc and Pit-2[13] in the BBM of proximal tubular segment[2,8] and therefore to increase the renal reabsorption of phosphate. The day of the experiment, in order to avoid lysosomal degradation, all rats were injected with 1 mg/100 g body weight of leupeptin (leupeptin trifluoractetate, Sigma, St Louis, MO, USA), from a stock of 20 mg/ml in saline as described previously[12,13]. After 30 min the animals received either saline as control, 5 µg/100 g body weight of PTH (PTH 1-34 fragment; Sigma, St Louis, MO, USA) or 1 µg/100 g body weight of recombinant human FGF-23 tagged C-terminally with the 6His epitope (rhFGF23 tyr25-ile251; R&D systems, Minneapolis, MN, USA). All substances were injected intraperitoneally. Rats were fixed by perfusion (see 4.2) at different time points (control and PTH animals 1h after injection, FGF-23-treated animals 2 h or 12h after injection).

Second experiment

This experiment was done with a total of 20 adult male Wistar rats weighing 150-250 g. As in the first one, rats were housed in a temperature-controlled environment with a 12-h light-dark circle with free access to water and food, and they were also kept 6 days in a low-phosphate diet (0.1% P_i content; Kliba AG, Switzerland). The rats were injected intraperitoneally with saline as control or with 1 µg/100 g body weight of rhFGF23 tagged C-terminally with the 6His epitope (rhFGF23 tyr25-ile251; R&D systems, Minneapolis, MN, USA). Before the injections, spot urine and sublingual blood samples with heparinized tubes were taken, although this was not possible for all the animals.

After the injections, rats were individually placed in metabolic cages for different time points: 2h, 6h and 18h for the FGF23-injected animals and 5h for the controls. The metabolic cages allow the exact measurement of food and water intake, body weight and separation and collection of faeces and urine as showed in the image (Figure 4.1.1). In this experiment, only urine samples were collected. In the urine collection tubes, protease inhibitor mix (thymol) and mineral oil was added to avoid the protein degradation and evaporation of the samples, respectively.

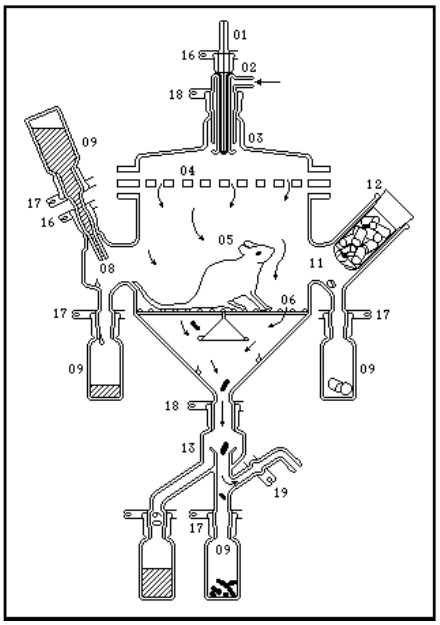

Figure 4.1.1: example of metabolic cage function[61].

After the indicated times, rats were anesthetized with isoflurane, their abdominal cavity was opened and the aorta and vena cava were exposed. Blood samples were taken with heparinized syringes from the vena cava, and then the rats were killed by cervical dislocation. Finally, femur, jejunum, duodenum, ilium and kidney samples were removed, immediately snap-frozen in liquid nitrogen, and transferred to a -80°C freezer until further use.

4.2 Fixation

In the first experiment, all animals were fixed by vascular perfusion. Rats were anesthetized with isofluorane and their abdominal/thoracic cavities were exposed. Animals were perfused via the left ventricle first with a prefixative solution (1000U/ml Heparin, 0.2% procain-HCl, 3.2% $CaCl_2$ and 0.18% NaCl), followed by perfusion with the fixative solution (3% paraformaldehyde in 0.1 M Na-cacodylate). After 5 min, kidneys were extracted and cut in halves, incubated for 2 hours in fixative solution followed by overnight incubation at 4°C in 32% sucrose/PBS. Kidneys were placed in embedding matrix (OCT) and were finally frozen in liquid propane cooled with liquid nitrogen.

4.3 Urine and blood sampling

Urine samples were centrifuged 7 min at 7000 rpm at room temperature. Then, supernatants were transferred to new tubes (always avoiding to take the pellet) and triplicates of 1:20 or 1:50 dilutions were done for measuring creatinine and phosphate concentrations, respectively. These tubes were stored at -20°C, whereas the rest of the undiluted urine stocks were stored at -80°C.

In the case of spot urine, the collection of samples for all animals was not possible.

Blood was collected with heparinized syringes and placed in heparinized tubes. Immediately after extraction, blood samples were centrifuged 7 min at 7000 rpm at 4°C to extract plasma. Plasma was snap-frozen in liquid nitrogen and stored at -80°C until further use.

4.4 Phosphate and creatinine determination

The Fiske and Subbarow's method was used to measure phosphate levels in plasma and urine samples. Urine precision control level 2 and Bovine serum assay control 1 (Randox Laboratories, Switzerland) were used as controls. The standard solution was 9.8 mM phosphate, from which several serial dilutions were done in sterile water in order to obtain the standard curve. For the colorimetric reaction to proceed, acid ammonium molybdate, Fiske and Subbarow reducer (Sigma-Aldrich, St Louis, MO, USA), and trichloroacetic acid were used. The intensity of the colorimetric reaction was measured in a spectrophotometer (BioTeK, Switzerland) at a wave length of 660 nm.

The Jaffe method was used to asses urinary creatinine concentration. For that, after incubating the urinary samples in a mixture of picric acid, sodium tetraborate and trisodium phosphate, the colorimetric intensity of the reaction was quantified in a spectrophotometer (BioTeK, Switzerland) at a wave length of 505 nm. The concentration of creatinine in urine was used to normalize the urinary phosphate values.

When serum phosphate levels are measured it's important to note that plasma phosphate levels are at their nadir in the morning and peak in the afternoon[45], so in our case all blood samples were recollected in the morning.

4.5 Measurements of FGF23 Levels

Human and rat FGF23 levels were measured in urine and/or plasma samples using a Human FGF23 (intact) and rat FGF23 (intact) ELISA Kits (Immutopics, San Clemente, CA, USA) following the manufacturer's instructions.

4.6 Immunohistochemistry

Frozen kidneys were cut using a cryomicrotome (Leica, Wetzlar, Germany) at -22°C. Serial sections, 5µm thick, were placed on slides (Superfrost Plus, Thermo Scientific) and kept in cold PBS until use.

Before addition of primary antibodies, renal sections were treated with blocking solution (1% bovine serum albumin in PBS) for 15 min, to prevent non-specific binding. After blocking, sections were incubated overnight at 4°C with either a mouse monoclonal anti-polyHistidine antibody (Sigma-Aldrich, St Louis, MO, USA), diluted 1:500 and 1:1000, that should recognize the His-tagged rhFGF23, or with a rabbit anti-rat antiserum against the NaPi-IIa protein diluted 1:1000[12,46]. In order to optimize the accessibility of the His-antibody, several antigen retrieval treatments were tested prior to addition of the antibody: 0.5% Sodium dodecyl sulfate in PBS for 5 min as well as 10mM Tris-Base (pH 10), sodium citrate buffer (pH 6) warmed up with a pressure cooker and 50mM ammonium chloride in PBS for 10 min. To test the specificity of the signal, some slices were incubated under the same conditions, but without primary antibodies.

After incubation with the primary antibodies, sections were rinsed two times with hypertonic solution and one time with PBS, then they were covered for 1h at 4°C with the secondary antibodies (Alexa Fluor 594 goat anti-mouse and anti-rabbit IgG (1:1000, Invitrogen, Carlsbad, CA, USA), as well as with FITC-phalloidin (1:100, Molecular probes, Eugene, OR, USA), and 4,6-diamidina-2-phenylindole (1:1000, DAPI; Sigma-Aldrich, St Louis, MO, USA). Primary and secondary antibodies were diluted in blocking solution. Finally the sections were rinsed two times with hypertonic solution and one time with PBS and covered with coverslips using DAKO-glycergel (DAKOpatts) containing

2.5% 1,4-diazabicyclo[2.2.2]octane (Sigma-Aldrich, St Louis, MO, USA) as a fading retardant. Slides were dried at 4°C for 1h.

Immunohistochemistry images were acquired with a Leica DM 6000 fluorescence microscope (Leica, Wetzlar, Germany) using equivalent exposure parameters for kidney sections stained with the same primary antibody.

4.7 Western Blot

Total proteins were extracted by homogenizing kidney tissue with RIPA extraction buffer [50 mM Tris-HCl, 150 mM NaCl, 1% NP-40, 0.5% deoxycholic acid sodium salt, 2 mM PMSF and protease inhibitor cocktail tablets (Roche, Basel, Switzerland)] using the Precellys 24 Homogenizer (Bertin Corp, Rockville, MD, USA) and MagNa Lyser Green Beads (Roche, Basel, Switzerland). The extracts were centrifuged at 13.000 rpm at 4°C for 15 min and the protein concentration of the supernatant was determined using DC Protein Assay Kit II (Bio-Rad, Hercules, CA, USA). Total protein samples (33 µg) were subjected to 10% SDS-PAGE in Criterion Empty Cassettes (26 well, 1mm; Bio-Rad, Hercules, CA, USA). Proteins were transferred to a polyvinylidene difluoride membrane (PVDF; Immobilon-P, Millipore) that was stained with Ponceau to check whether the transfer had worked. After blocking for 30 min at room temperature in blocking solution (5% fat-free powder milk in Tris-buffered saline containing 0.1% Tween-20), the membranes were incubated overnight at 4°C with the primary antibodies: rabbit polyclonal antibody against Cyp24A1 (1:1000; proteintech, Chicago, IL, USA), mouse monoclonal antibody against VDR (1:500, Santa Cruz Biotechnology, Dallas, TX, USA), and rabbit polyclonal antibody against NaPi-IIa (1:5000; homemade: Custer et al, 1994). Membranes were washed with Tris-buffered saline, blocked 20 min at room temperature with blocking solution and covered for 2 h at room temperature with the secondary antibodies: donkey anti-rabbit IgG Horseradish Peroxidase-linked, whole antibody (1:10000; Healthcare Life Sciences, Little Chalfont, Buckinghamshire, UK) or sheep anti-mouse IgG Horseradish Peroxidase-linked, F(ab')2 fragment (1:10000; Healthcare Life Sciences, Little Chalfont, Buckinghamshire, UK). Both primary and secondary antibodies were diluted in blocking solution. Finally, the membranes were washed with Tris-buffered saline and incubated for 5 min at room temperature with the chemiluminescence substrate (Immobilon Western Chemiluminescent HRP substrate;

Merck Millipore, Billerica, MA, USA). Signals were acquired using a LAS-4000 camera (Fujifilm).

Upon signal acquisition, antibodies were stripped from the PVDF membranes by incubation for 30 minutes at room temperature in a stripping solution containing 25 mM Glycine, 1% SDS, pH adjusted to 2 with HCl. After stripping, the membrane was incubated with a mouse IgG2a isotype monoclonal anti-polyHistidine (1:3000; Sigma-Aldrich, St Louis, MO, USA) that should recognize the His-epitope in the rhFGF23. Sheep anti-mouse IgG Horseradish Peroxidase-linked, F(ab')2 fragment (1:10000; Healthcare Life Sciences, Little Chalfont, Buckinghamshire, UK) was used as secondary antibody. Then, the membrane was processed for chemiluminiscence determination as indicated above.

Finally, membranes were striped and probed with a mouse monoclonal anti-β-actin antibody (1:12000; Abcam, Cambridge, UK), and donkey anti-mouse IgG Horseradish Peroxidase-linked, whole antibody as secondary antibody (1:10000; Healthcare Life Sciences, Little Chalfont, Buckinghamshire, UK). Actin was used as a loading control and the subsequent analysis of the proteins of interest were determined as relative abundance to β-actin (protein of interest/ β-actin).

4.7.1 Anti-polyHistidine antibody validation

Plasma samples from saline-injected animals (0 pg rhFGF23), FGF-injected animals sacrificed 2 hours post-injection (1455 pg rhFGF23) as well as 100 ng of pure His-tagged rhFGF23 were subjected to a 12% SDS-PAGE. PVDF membranes were incubated with a mouse monoclonal anti-polyHistidine antibody (Sigma-Aldrich, St Louis, MO, USA) using the same protocol described above. Both sheep anti-mouse IgG Horseradish Peroxidase-linked, F(ab')2 fragment (1:10000; Healthcare Life Sciences, Little Chalfont, Buckinghamshire, UK) and donkey anti-mouse IgG (H+L), AP conjugate (1:5000; Promega, Madison, WI, USA) were used as secondary antibodies.

4.8 RNA isolation, RT-PCR and quantitative real-time PCR

Frozen kidneys were homogenized using the Precellys 24 Homogenizer (Bertin Corp, Rockville, MD, USA) and MagNa Lyser Green Beads (Roche, Basel, Switzerland), and RNA was immediately extracted using RNeasy micro kit (QIAGEN, Hilden, Germany) according to the manufacturer's instructions. DNase digestion was performed using the RNase-free DNase Set (QIAGEN, Hilden, Germany). Total RNA extractions were quantified using the NanoDrop ND-1000 spectrophotometer (Wilmington, DE, USA). cDNA was prepared from diluted RNA samples (100 ng/µl) using TaqMan Reverse Transcriptase reagent Kit containing 10x RT buffer, $MgCl_2$ random hexamers, dNTPs, RNAse inhibitors and Multiscribe reverse transcriptase (Applied Biosystems/Roche, Forster City, CA, USA). Thermocycling conditions for reverse transcription were set at 25°C for 10 min, 48°C for 30 min, and 95°C for 5 min (Biometra TGradient thermocycler, Goettingen, Germany). The samples were stored at -20°C until use. Real-time PCR was used to determine relative mRNA expression (7500 Fast Real-Time PCR system, Applied Biosystems). Thermocycling conditions were as follows: initial denaturation at 95°C for 10 min, followed by 40 cycles of 95°C for 15 sec and 60°C for 1 min. Forward and reverse primer concentration was 25 µM; probe concentration was 5 µM. The primers and probe sequences for NaPi-IIa were: 5'-GGA ATC ACA GTC TCA TTC GGA TT-3', forward; 5'-ATG GCC TCT ACC CTG GAC ATA G-3', reverse; 5'-TGT CAA CCA GAG ACA AAA GAG GCT TCC ACT-3', probe. Probes were generated with the reporter dye FAM at the 5' end and TAMRA at the 3' end. Each sample was run in triplicate including a negative control (untranscribed RNA). The cycle threshold (C_t) values obtained were ultimately compared to C_t values of the house keeping gene 18S. Relative mRNA expression ratios were calculated as $R=2^{[Ct(18S)-Ct(gene\ of\ interest)]}$.

4.9 Statistical analysis

All data was analyzed using Bonferroni's multiple comparison test with only p values $\leq$ 0.05 considered as statistically significant.

5. Results

5.1 FGF23 plasma levels (first experiment)

Measurements of recombinant human FGF23 plasma levels in the first experimental group showed that in the animals sacrificed 2 h after the rhFGF23 injection, the human FGF23 was clearly detected (Figure 5.2.1a) demonstrating that the intraperitoneally injection worked properly. The decrease after 12 h (overnight group) is probably due to the metabolization of the rhFGF23 during this time. Injected of rhFGF23 induced no changes on the endogenous FGF23 (Figure 5.2.1b).

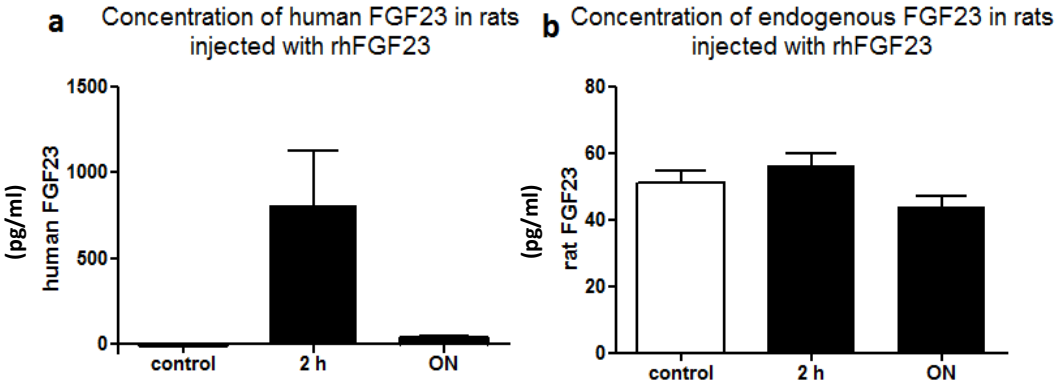

Figure 5.2.1: (a) Plasma levels of human FGF23 2 and 12 hours (ON) after rhFGF23 injection and in the control group. 2 h (n = 4), overnight (n = 4), and control (n = 4). **(b)** Plasma endogenous rat FGF23 levels in the same groups of rats. 2 h (n = 4), overnight (n = 4), and control (n = 4).

5.2 Immunohistochemistry (first experiment)

Incubation of kidney slices with an anti-His antibody that should recognized the His-tagged injected FGF23 resulted in no signal, although a large number of antigen retrieval treatments were tested (data not shown).

His-tag antibody validation

We had to discard the possibility that immunohistochemistry signal for rhFGF23 was negative because of the lack of sensitivity/degradation of the used primary antibody. Therefore, we did a western blot in which we load pure rhFGF23 (the same that was injected to the rats) and the membranes were incubated with the same primary antibody used in the slides. This experiment was also negative, although we tried to develop it with

different secondary antibodies either conjugated to alkaline phosphatase or to horseradish peroxidase (data not shown).

5.3 Human FGF23 levels in urine and plasma (second experiment)

We analyzed the recombinant human FGF23 levels in plasma and urine samples (Figure 5.3.1a, b) collected at different time points after the injections.

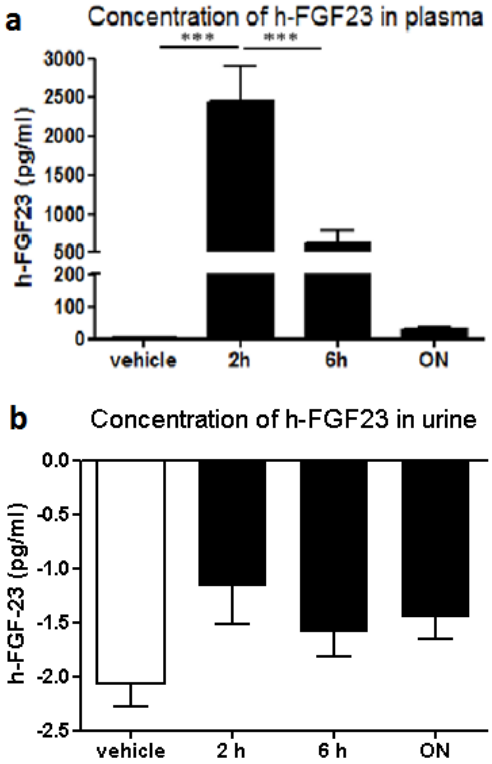

Figure 5.3.1: (a) Plasma levels of human FGF23 in blood samples collected at different time points (2 h, 6 h or18 h (ON)) after injection and vehicle group. Vehicle (n = 5), 2 h (n = 5), 6 h (n = 5) and overnight (n = 5).**(b)** Urine levels of human FGF23 levels in samples recollected at the same time points as above. Vehicle (n = 5), 2 h (n = 2), 6 h (n = 5) and overnight (n = 5). ***p < 0.001.

In plasma, the highest concentration of rhFGF23 was detected two hours after application, whereas six hours later the levels decreased significantly. In agreement with the first experiment, 18 h after the injection (ON) the levels were reduced to almost background.

On the other hand, we were not able to detect human FGF23 in urine samples at any time point.

5.4 Inorganic phosphate levels

As shown in Figure 5.4.1a, the phosphate plasma levels remained stable and equal to the control group (≈2mM) indicating that there was no effect on the plasma phosphate levels due to the FGF23 injection.

However, we observed that the injections had an effect on the urinary phosphate excretion (Figure 5.4.1b). The urinary phosphate levels remain stable during the first 2 h. Then they increase in samples collected during the 6 h after the injection, although due to the high scatter of the values the change did

not reached statistical significance. Urinary phosphate in samples collected during the next 18 h post-injection (ON) show not differences compared with the vehicle treated group.

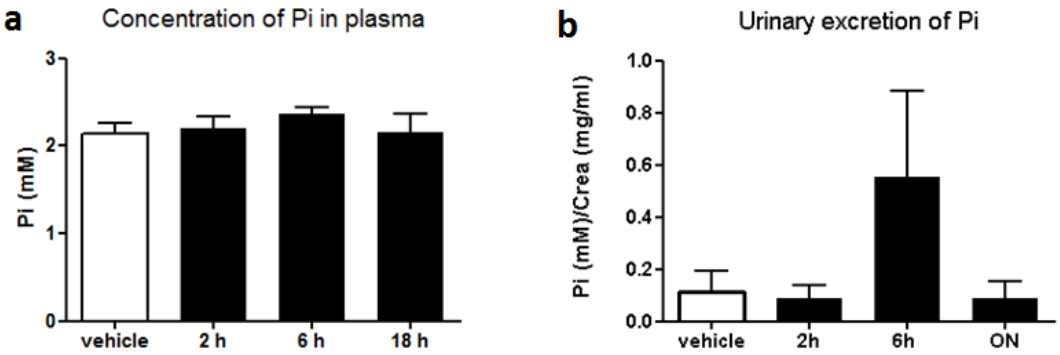

Figure 5.4.1: (a) Concentration of Pi in plasma samples obtained at different time points (2 h, 6 h or 18 h (ON) t) after IP rhFGF23 injections and in the control group. vehicle (n = 5), 2 h (n = 5), 6 h (n = 5) and overnight (n = 5) **(b)** Urinary Pi measurements in urine collected during different time points (2 h, 6 h or 18 (ON)) after rhFGF23 injections and in the control group. Vehicle (n = 4), 2 h (n = 2), 6 h (n = 5) and overnight (n = 5).

5.5 qPCR

It has been previously shown that FGF23 reduces the expression of NaPi-IIa in the apical brush border membrane from proximal tubular cells in the kidney[5,6,18,20,24,26,47,48]. As shown in figure 5.5.1, NaPi-IIa mRNA expression remained unaffected 2 h after FGF23 injection, but was markedly decreased in the 6 h group. In rats kept overnight, the mRNA levels are increased compared with the 6 h group.

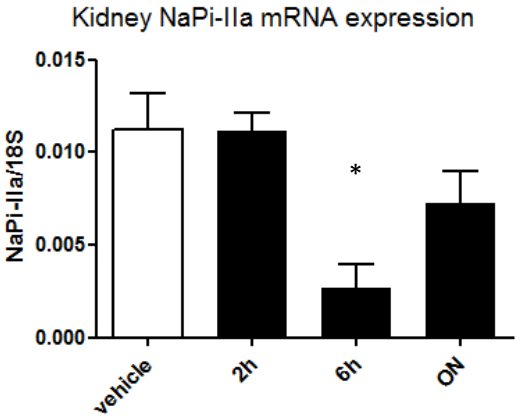

Figure 5.5.1: NaPi-IIa mRNA expression 2 h, 6 h or 18 h after IP rhFGF23 injection and in control group. RNA was extracted from total kidney homogenates and mRNA expression was determined by quantitative real-time RT-PCR. Vehicle (n = 5), 2 h (n = 4), 6 h (n = 5) and overnight (n = 5).*$p < 0.05$.

5.6 Immunoblotting

We prepared total protein extractions from kidney for immunoblotting to examine the relative abundance of rhFGF23NaPi-IIa, Cyp24a1, and VDR after 2 h, 6 h and 18 h (ON) after rhFGF23 application (Figure 5.6.1a, b). The expression of Cyp24a1 tended to increase in the 6 and 18 h groups, but the changes were not significant. Instead, the

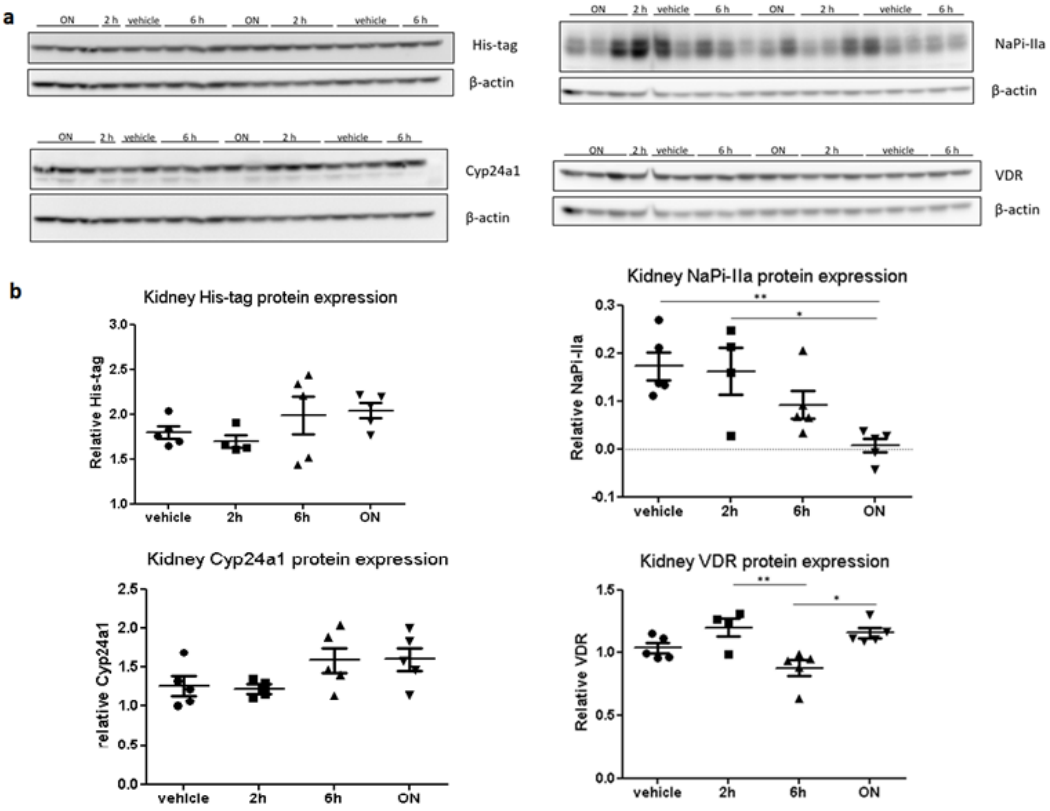

Figure 5.6.1: Total proteins were obtained from kidney tissue and 33 µg were loaded per lane for immunoblotting (n = 5 per group, excluding 2 h group in which n = 4). **(a)** Membranes were initially tested for Cyp24a1 and NaPi-IIa , and stripped to reprobe for β-actin to control for loading. Two membranes were stripped again and incubated with an anti-VDR antibody and an anti His-tag antibody **(b)** Densitometric analysis of membranes was performed, and the bands of the proteins of interest were normalized against β-actin. Vehicle (n = 5), 2 h (n = 4), 6 h (n = 5) and overnight (n = 5) *p < 0.05, **p < 0.01.

abundance of NaPi-IIa progressively decreases although due to the scatter of the data statistical significance was only reached in the 18 h group. The abundance of the VDR showed a transient reduction in the 6 h group, returning to vehicle-treated levels 18 h after FGF23 administration. Moreover, there is a problem in the His-tag membrane, expression can be observed in the control group, in which no rhFGF23 was injected. Thus, this results are not valid.

6. Discussion

We first studied whether the kidney plays a role in the regulation of FGF23 metabolism. We hypothesized, that the kidney filtrates, reabsorbs and degrades plasma FGF23 because when Mace and colleagues did kidney nephrectomy in rats they observed that FGF23 plasma levels increased and that in intact rats there was more FGF23 entering the kidney through the artery as leaving it in the vein[44]. To test our hypothesis, we injected rhFGF23 tagged with a 6His-epitope; the tagging allow us to use a well characterized monoclonal antibody to detect FGF23 by immunofluorescence/Western blot. To prevent a potential lysosomal degradation, lysosomal proteases were inhibited prior to rhFGF23 administration.

We first validated our experimental FGF23 administration protocol by measuring the plasma concentration of rhFGF23 at several time-points after administration. These determinations consistently showed that the maximal levels of rhFGF23 are detected 2 h post-injection, gradually decreasing thereafter, whereas no signal was detected in vehicle injected rats. These results indicate that IP injections worked, so if FGF23 is somehow degraded in the kidney cells it should be detected by immunohistochemistry. However, no FGF23-related signal (His-signal) was observed in kidneys collected 2 or 12 hours post-injection. A problem with the interpretation of this data is that we lack a positive control; furthermore, several attempts on validating the specificity of the His antibody on western blot were unsuccessful either due to technical problems (inappropriate substrate for chemiluminesce or insufficient stripping) or to the lack of accessibility. In this regard, it has been described that this antibody validation technique can have some limitations; proteins are denatured in SDS, and so they lose their secondary and tertiary structure. Some antibodies bind only to native proteins in immunohistochemistry, and some antibodies only bind to denatured protein in immunoblots[49]. As in the data sheet of the His antibody it has been described its use for both immunoblotting and immunofluorescent staining it's very improbable that this could be a problem. Therefore, the immunofluorescence experiments should be repeated before any conclusion is withdrawn.

There are some discrepancies about the half-life of FGF23. The half-life of plasma iFGF23 in humans is in the range of 46-58 min in tumor-induced osteomalacia[50], in contrast to another study in which the circulating half-life of FGF23 was 21.5 min in TIO patients[51]. In

experimental studies in animals, estimated half-life varied from 4.4 min to 22 min[44,52]. In these cases, the FGF23 was injected intravenously whereas in the present study intraperitoneal administration was used, in which absorption of material delivered is typically much slower[53]., Although no half-life was calculated in our study, the injected FGF23 starts to degrade between 2 and 6 h after the injection, so if the kidney filtrates and reabsorbs FGF23 same FGF23-related signal should be detected between this time points.

On the other hand, the molecular weight cutoff for glomerular filtration is thought to be 30 – 50 kDa[54,55], but it also depends on the molecular charge and shape[56]. Albeit FGF23 is a 32 kDa protein[16,18,44], it's not known if it undergoes glomerular filtration. Moreover, if filtrated, FGF23 may or may not be reabsorbed and in the latest case it would be excreted with the urine. However, we could no detect the presence of FGF23 in urine samples at any time point post-administration.

In our second study rhFGF23 was again injected into rats but we added a new intermediate time point for sampling (between the 2 and 12 h) we collected organs implicated in the metabolism of phosphate, and we focused on the time-course of the effect of FGF23 on phosphate-related parameters.

As expected, FGF23 injection resulted in an enhanced urinary phosphate excretion; increase phosphaturia was first detected 6h after injection. As previously mentioned, the transporter responsible for the bulk of Pi reabsorption in the renal proximal tubules is NaPi-IIa[2,8,11,12,16], and its expression is decreased by FGF23[8]. Therefore we studied the mRNA and protein expression of this transporter in the extracted kidney tissue. In concordance with the excreted Pi data, both the NaPi-IIa mRNA and protein expression were reduced after 6 h. Taken together these results indicate that the mechanism of action of FGF23 in the kidney probably takes place in this range of time (2 to 6 h). This is far slower than the effect of PTH, since upon IP injection in rats, changes on NaPi-IIa expression were reported as early as 15 min after PTH administration[57]. At 6 hours postadministration, the changes in NaPi-IIa expression were larger at the mRNA than protein level, which makes sense because transcriptional regulation is not immediate. In rats that were kept overnight after the injection, phosphaturia had normalized despite persistent downregulation of NaPi-IIa. Lack of correlation between urinary excretion of phosphate and NaPi-IIa abundance was also reported upon PTH administration to rats[58].

Despite the above mentioned changes on urinary phosphate, the levels of phosphate in plasma remained unaltered and equal to control group in all the time points. Expected was that that plasma Pi levels decreased, as high FGF23 levels are related with hypophosphtemia[16,59]. This suggests a compensatory mechanism that maintains the homeostasis. There are reported cases in which lower dietary phosphate absorption result in 24-hour urinary phosphate excretion while serum phosphate levels remain unchanged[45].

As FGF23 and vitamin D maintain negative feedback loops, is not surprising that the VDR protein expression is significantly reduced after 6 h of FGF23 injection. The reported pathway that leads to $1,25(OH)_2D_3$/calcitriol reduction by FGF23 is the induction of CYP24a1 that leads to degradation of 25OHD and 1,25OHD[18,35], and suppression of CYP27b1 blocking $1,25(OH)_2D_3$ synthesis. Surprisingly, no enhanced CYP24a1 protein levels are found. To study further this effect both calcitriol and CYP27b1 levels should be analyzed.

7. Conclusions

The effects of FGF23 on phosphate metabolism are primarily 6 h after rhFGF23 injection. As expected, this rapid increase in FGF23 plasma levels lead to a decrease of the NaPi-IIa cotransporter, which stimulated the renal excretion of Pi increasing the urinary phosphate levels.

To completely understand the time-course of the action of FGF23 in phosphate handling, further experiments should be done, including the study of other organs like intestine or bones.

Moreover, no evidences for FGF23 kidney clearance could be founded. Although there were some technical problems, no conclusions can be extracted from our immunofluorescence assays, our data is consistent with the absence of urinary excretion of FGF23.

8. Bibliography

1. Bergwitz, C. & Jüppner, H. Regulation of phosphate homeostasis by PTH, vitamin D, and FGF23. *Annu. Rev. Med.* **61,** 91–104 (2010).

2. Wagner, C. A., Hernando, N., Forster, I. C. & Biber, J. The SLC34 family of sodium-dependent phosphate transporters. *Pflugers Archiv European Journal of Physiology* **466,** 139–153 (2014).

3. Jüppner, H. Phosphate and FGF-23. *Kidney Int.* **79121,** S24–7 (2011).

4. Sapir-Koren, R. & Livshits, G. Bone mineralization is regulated by signaling cross talk between molecular factors of local and systemic origin: the role of fibroblast growth factor 23. *Biofactors* **40,** 555–68

5. Fernandes-freitas, I. & Owen, B. M. ScienceDirect Metabolic roles of endocrine fibroblast growth factors. 30–35 (2015).

6. Donate-Correa, J., Muros-de-Fuentes, M., Mora-Fernández, C. & Navarro-González, J. F. FGF23/Klotho axis: Phosphorus, mineral metabolism and beyond. *Cytokine Growth Factor Rev.* **23,** 37–46 (2012).

7. Biber, J., Murer, H., Mohebbi, N. & Wagner, C. A. Renal handling of phosphate and sulfate. *Compr. Physiol.* **4,** 771–92 (2014).

8. Tatsumi, S. *et al.* Regulation of renal phosphate handling: inter-organ communication in health and disease. *J. Bone Miner. Metab.* **34,** 1–10 (2016).

9. Lederer, E. Regulation of serum phosphate. *J. Physiol.* **592,** 3985–95 (2014).

10. Sabbagh, Y., Giral, H., Caldas, Y., Levi, M. & Schiavi, S. C. Intestinal phosphate transport. *Adv. Chronic Kidney Dis.* **18,** 85–90 (2011).

11. Biber, J., Hernando, N. & Forster, I. Phosphate transporters and their function. *Annu. Rev. Physiol.* **75,** 535–50 (2013).

12. Picard, N. *et al.* Acute parathyroid hormone differentially regulates renal brush border

membrane phosphate cotransporters. *Pflügers Arch. Eur. J. Physiol.* **460,** 677–87 (2010).

13. Bacic, D. *et al.* The renal Na+/phosphate cotransporter NaPi-IIa is internalized via the receptor-mediated endocytic route in response to parathyroid hormone. *Kidney Int.* **69,** 495–503 (2006).

14. Hernando, N. *et al.* NaPi-IIa and interacting partners. *J. Physiol.* **567,** 21–6 (2005).

15. Bhattacharyya, N., Chong, W. H., Gafni, R. I. & Collins, M. T. Fibroblast growth factor 23: state of the field and future directions. *Trends Endocrinol. Metab.* **23,** 610–8 (2012).

16. Hu, M. C., Shiizaki, K., Kuro-o, M. & Moe, O. W. Fibroblast growth factor 23 and Klotho: physiology and pathophysiology of an endocrine network of mineral metabolism. *Annu. Rev. Physiol.* **75,** 503–33 (2013).

17. Liu, S. & Quarles, L. D. How Fibroblast Growth Factor 23 Works. *J. Am. Soc. Nephrol.* **18,** 1637–1647 (2007).

18. Quarles, L. D. Role of FGF23 in vitamin D and phosphate metabolism: implications in chronic kidney disease. *Exp. Cell Res.* **318,** 1040–8 (2012).

19. van der Meijden, K. *et al.* Regulation of CYP27B1 mRNA Expression in Primary Human Osteoblasts. *Calcif. Tissue Int.* (2016). doi:10.1007/s00223-016-0131-9

20. Wolf, M. & White, K. E. Coupling fibroblast growth factor 23 production and cleavage: iron deficiency, rickets, and kidney disease. *Curr. Opin. Nephrol. Hypertens.* **23,** 411–9 (2014).

21. Guo, Y.-C. & Yuan, Q. Fibroblast growth factor 23 and bone mineralisation. *Int. J. Oral Sci.* **7,** 8–13 (2015).

22. Smith, E. R., McMahon, L. P. & Holt, S. G. Fibroblast growth factor 23. *Ann. Clin. Biochem.* **51,** 203–27 (2014).

23. Kovesdy, C. P. & Quarles, L. D. Fibroblast growth factor-23: what we know, what we don't know, and what we need to know. *Nephrol. Dial. Transplant* **28,** 2228–36 (2013).

24. Quarles, L. D. Skeletal secretion of FGF-23 regulates phosphate and vitamin D metabolism. *Nat. Rev. Endocrinol.* **8,** 276–86 (2012).

25. Martin, A., David, V. & Quarles, L. D. Regulation and function of the FGF23/klotho endocrine pathways. *Physiol. Rev.* **92,** 131–55 (2012).

26. Yan, X. *et al.* Fibroblast growth factor 23 reduces expression of type IIa Na+/Pi co-transporter by signaling through a receptor functionally distinct from the known FGFRs in opossum kidney cells. *Genes to Cells* **10,** 489–502 (2005).

27. Ureña-Torres, P. *et al.* Association of kidney function, vitamin D deficiency, and circulating markers of mineral and bone disorders in CKD. *Am. J. Kidney Dis.* **58,** 544–53 (2011).

28. van Ballegooijen, A. J., Rhee, E. P., Elmariah, S., de Boer, I. H. & Kestenbaum, B. Renal Clearance of Mineral Metabolism Biomarkers. *J. Am. Soc. Nephrol.* **27,** 392–7 (2016).

29. Christakos, S., Ajibade, D. V, Dhawan, P., Fechner, A. J. & Mady, L. J. Vitamin D: metabolism. *Endocrinol. Metab. Clin. North Am.* **39,** 243–53, table of contents (2010).

30. Bikle, D. D. Vitamin D Metabolism, Mechanism of Action, and Clinical Applications. *Chem. Biol.* **21,** 319–329 (2014).

31. Ross, A. C., Taylor, C. L., Yaktine, A. L. & Valle, H. B. Del. Overview of Vitamin D. (2011).

32. Lin, R. Crosstalk between Vitamin D Metabolism, VDR Signalling, and Innate Immunity. *Biomed Res. Int.* **2016,** 1375858 (2016).

33. Kulie, T., Groff, A., Redmer, J., Hounshell, J. & Schrager, S. Vitamin D: An Evidence-Based Review. *J. Am. Board Fam. Med.* **22,** 698–706 (2009).

34. Tieu, E. W., Tang, E. K. Y. & Tuckey, R. C. Kinetic analysis of human CYP24A1 metabolism of vitamin D via the C24-oxidation pathway. *FEBS J.* **281,** 3280–96 (2014).

35. Haussler, M. R. *et al.* The role of vitamin D in the FGF23, klotho, and phosphate bone-kidney endocrine axis. *Rev. Endocr. Metab. Disord.* **13,** 57–69 (2012).

36. Amling, M. *et al.* Rescue of the skeletal phenotype of vitamin D receptor-ablated mice in the setting of normal mineral ion homeostasis: formal histomorphometric and biomechanical analyses. *Endocrinology* **140,** 4982–7 (1999).

37. DeLuca, H. F. The metabolism and functions of vitamin D. *Adv. Exp. Med. Biol.* **196,** 361–75 (1986).

38. Nair, R. & Maseeh, A. Vitamin D: The "sunshine" vitamin. *J. Pharmacol. Pharmacother.* **3,** 118–26 (2012).

39. Aranow, C. Vitamin D and the immune system. *J. Investig. Med.* **59,** 881–6 (2011).

40. Hattenhauer, O., Traebert, M., Murer, H. & Biber, J. Regulation of small intestinal Na-P(i) type IIb cotransporter by dietary phosphate intake. *Am. J. Physiol.* **277,** G756–62 (1999).

41. Baum, M. The bone kidney axis. *Curr. Opin. Pediatr.* **26,** 177–9 (2014).

42. Kumar, R., Tebben, P. J. & Thompson, J. R. Vitamin D and the kidney. *Arch. Biochem. Biophys.* **523,** 77–86 (2012).

43. Henry, H. L. *et al.* Regulation of vitamin D metabolism. *Best Pract. Res. Clin. Endocrinol. Metab.* **25,** 531–541 (2011).

44. Mace, M. L., Gravesen, E., Hofman-Bang, J., Olgaard, K. & Lewin, E. Key role of the kidney in the regulation of fibroblast growth factor 23. *Kidney Int.* **88,** 1304–1313 (2015).

45. Isakova, T. *et al.* Rationale and Approaches to Phosphate and Fibroblast Growth Factor 23 Reduction in CKD. *J. Am. Soc. Nephrol.* **26,** 2328–39 (2015).

46. Custer, M., Lötscher, M., Biber, J., Murer, H. & Kaissling, B. Expression of Na-P(i) cotransport in rat kidney: localization by RT-PCR and immunohistochemistry. *Am. J. Physiol.* **266,** F767–74 (1994).

47. Gattineni, J. *et al.* FGF23 decreases renal NaPi-2a and NaPi-2c expression and induces hypophosphatemia in vivo predominantly via FGF receptor 1. *AJP Ren. Physiol.* **297,** F282–F291 (2009).

48. Razzaque, M. S. The FGF23-Klotho axis: endocrine regulation of phosphate homeostasis. *Nat. Rev. Endocrinol.* **5,** 611–9 (2009).

49. Burry, R. W. Controls for immunocytochemistry: an update. *J. Histochem. Cytochem.* **59,** 6–12 (2011).

50. Khosravi, A. *et al.* Determination of the Elimination Half-Life of Fibroblast Growth Factor-23. *J. Clin. Endocrinol. Metab.* **92,** 2374–2377 (2007).

51. Takeuchi, Y. *et al.* Venous sampling for fibroblast growth factor-23 confirms preoperative diagnosis of tumor-induced osteomalacia. *J. Clin. Endocrinol. Metab.* **89,** 3979–82 (2004).

52. Christov, M. *et al.* Plasma FGF23 levels increase rapidly after acute kidney injury. *Kidney Int.* **84,** 776–85 (2013).

53. Turner, P. V, Brabb, T., Pekow, C. & Vasbinder, M. A. Administration of substances to laboratory animals: routes of administration and factors to consider. *J. Am. Assoc. Lab. Anim. Sci.* **50,** 600–13 (2011).

54. Ruggiero, A. *et al.* Paradoxical glomerular filtration of carbon nanotubes. *Proc. Natl. Acad. Sci. U. S. A.* **107,** 12369–74 (2010).

55. Liu, J., Yu, M., Zhou, C. & Zheng, J. Renal clearable inorganic nanoparticles: a new frontier of bionanotechnology. *Mater. Today* **16,** 477–486 (2013).

56. Haraldsson, B., Nyström, J. & Deen, W. M. Properties of the glomerular barrier and mechanisms of proteinuria. *Physiol. Rev.* **88,** 451–87 (2008).

57. Lötscher, M. *et al.* Rapid downregulation of rat renal Na/P(i) cotransporter in response to parathyroid hormone involves microtubule rearrangement. *J. Clin. Invest.* **104,** 483–94 (1999).

58. Friedlaender, M. M., Wald, H., Dranitzky-Elhalel, M., Levi, M. & Popovtzer, M. M. Recovery of renal tubule phosphate reabsorption despite reduced levels of sodium-phosphate transporter. *Eur. J. Endocrinol.* **151,** 797–801 (2004).

59. Saito, T. *et al.* Fibroblast Growth Factor 23 (FGF23) and Disorders of Phosphate Metabolism. *Int. J. Pediatr. Endocrinol.* **2009,** 1–6 (2009).

60. Shaker, J. L. & Deftos, L. *Calcium and Phosphate Homeostasis*. *Endotext* (2000).

61. International Program on Chemical Safety., United Nations Environment Programme., International Labour Organisation. & World Health Organization. *Principles of toxicokinetic studies.* (World Health Organization, 1986).